1521-0103/349/2/248–257$25.00
THE JOURNAL OF PHARMACOLOGY AND EXPERIMENTAL THERAPEUTICS

http://dx.doi.org/10.1124/jpet.113.208728
J Pharmacol Exp Ther 349:248–257, May 2014

Novel Curcumin Derivative CNB-001 Mitigates Obesity-Associated Insulin Resistance[S]

Evgeniy Panzhinskiy, Yinan Hua, Paul A. Lapchak, Elena Topchiy, Teresa E. Lehmann, Jun Ren, and Sreejayan Nair

Division of Pharmaceutical Sciences and Center for Cardiovascular Research and Alternative Medicine, University of Wyoming, College of Health Sciences, Laramie, Wyoming (E.P., Y.H., J.R., S.N.); Cedars-Sinai Medical Center, Department of Neurology and Neurosurgery, Burns and Allen Research Institute, Los Angeles, California (P.A.L.); and Chemistry Department, University of Wyoming, Laramie, Wyoming (E.T., T.E.L.)

Received August 13, 2013; accepted February 13, 2014

ABSTRACT

Type 2 diabetes is growing at epidemic proportions, and pharmacological interventions are being actively sought. This study examined the effect of a novel neuroprotective curcuminoid, CNB-001 [4-((1*E*)-2-(5-(4-hydroxy-3-methoxystyryl-)-1-phenyl-1*H*-pyrazoyl-3-yl)vinyl)-2-methoxy-phenol], on glucose intolerance and insulin signaling in high-fat diet (HFD)–fed mice. C57BL6 mice (5–6 weeks old) were randomly assigned to receive either a HFD (45% fat) or a low-fat diet (LFD, 10% fat) for 24 weeks, together with CNB-001 (40 mg/kg i.p. per day). Glucose tolerance test revealed that the area under the curve of postchallenge glucose concentration was elevated on HF-feeding, which was attenuated by CNB-001. CNB-001 attenuated body weight gain, serum triglycerides, and IL-6, and augmented insulin signaling [elevated phosphoprotein kinase B (p-Akt), and phosphoinsulin receptor (p-IR)β, lowered endoplasmic reticulum (ER) stress, protein–tyrosine phosphatase 1B (PTP1B)] and glucose uptake in gastrocnemius muscle of HFD-fed mice. Respiratory quotient, measured using a metabolic chamber, was elevated in HFD-fed mice, which was unaltered by CNB-001, although CNB-001 treatment resulted in higher energy expenditure. In cultured myotubes, CNB-001 reversed palmitate-induced impairment of insulin signaling and glucose uptake. Docking studies suggest a potential interaction between CNB-001 and PTP1B. Taken together, CNB-001 alleviates obesity-induced glucose intolerance and represents a potential candidate for further development as an antidiabetic agent.

Introduction

Obesity is a growing epidemic worldwide and is considered to be a major public health threat (Ogden et al., 2007). Obesity underlies the development of metabolic syndrome and type 2 diabetes, which are the major risk factors for cardiovascular disease, the leading cause of morbidity and mortality in developed countries (Bahrami et al., 2008). Insulin resistance, characterized as the failure of the body to respond to the normal actions of the hormone insulin, has been recognized as a fundamental aspect in the etiology of type 2 diabetes and has been observed years before the development of full-blown diabetes (Kahn and Flier, 2000). Thus, insulin resistance serves as a potential therapeutic target to prevent and preempt complications associated with obesity. Therefore, identification and characterization of insulin-sensitizing agents play a key role in the treatment of obesity-related metabolic disorders.

Curcumin is a natural polyphenolic compound that is responsible for the yellow color of the popular Indian spice turmeric obtained from herb *Curcuma longa*. It has shown diverse pharmacological properties including antioxidant, anticarcinogenic, antiangiogenic, antiproliferative, and anti-inflammatory activities (Aggarwal et al., 2007). Curcumin has been described as a potential glucose-lowering agent and antioxidant in type 2 diabetic mice (Seo et al., 2008). Animal studies have shown the beneficial effects of curcumin on hyperlipidemia and insulin resistance caused by high-fat diet feeding (Shao et al., 2012). Prevention of hepatic steatosis by

This work was supported in part by the National Institutes of Health National Center for Research Resources [Grant P20-RR016474]; and the National Institutes of Health National Institute of General Medical Sciences [Grant P20-GM103432] (to S.N. and J.R.); the National Institutes of Health National Institute of General Medical Sciences Wyoming INBRE Bioinformatics Core [Grant 8P20-GM103432] (to S.N.); and the National Institutes of Health National Institute of Neurologic Disorders and Stroke [Grant U01-NS060685] (to P.A.L.). S.N. is the guarantor of this work, had full access to all the data, and takes full responsibility for the integrity of data and the accuracy of data analysis.

Portions of this article were presented: Panzhinskiy E, Lapchak PA, Ren J, and Nair S (2012) A novel neuroprotective curcuminoid alleviates glucose intolerance and improves insulin signaling. *FASEB J* **26:**672.7; *Experimental Biology 2012*; 21–25 Apr 2012; San Diego, CA, for which E.P. received the travel award from ASPET.

dx.doi.org/10.1124/jpet.113.208728.

[S] This article has supplemental material available at jpet.aspetjournals.org.

ABBREVIATIONS: Akt, protein kinase B; AUC, area under the curve; CNB-001, 4-((1*E*)-2-(5-(4-hydroxy-3-methoxystyryl-)-1-phenyl-1*H*-pyrazoyl-3-yl)vinyl)-2-methoxy-phenol); DMEM, Dulbecco's modified Eagle's medium; eIF2α, eukaryotic initiation factor 2α; ER, endoplasmic reticulum; GAPDH, glyceraldehyde-3-phosphate dehydrogenase; GRP78, glucose-regulated protein 78; HFD, high-fat diet; IPITT, intraperitoneal insulin tolerance test; IPGTT, intraperitoneal glucose tolerance test; IR, insulin receptor; IRS-1, insulin receptor substrate-1; MTT, 3-(4,5-dimethylthiazol-2-yl)-2,5-diphenyltetrazolium; ND, normal diet; PA, palmitic acid; PTP1B, protein–tyrosine phosphatase 1B; RER, respiratory exchange ratio.

curcumin in fructose-fed rats has been described recently (Li et al., 2010). Several mechanisms have been proposed for the aforementioned beneficial effects of curcumin, including inhibition of nuclear factor κB and mammalian target of rapamycin (mTOR) pathways, activation of peroxisome proliferator–activated receptor (PPAR)γ, reduction of obesity-associated endoplasmic reticulum (ER) stress (Alappat and Awad, 2010), and inhibition of acetyltransferase (Balasubramanyam et al., 2004). However, instability in vivo and poor bioavailability limits the development of curcumin for therapy (Anand et al., 2007). Recent studies have identified the novel curcumin derivative CNB-001 [4-((1*E*)-2-(5-(4-hydroxy-3-methoxystyryl-)-1-phenyl-1*H*-pyrazoyl-3-yl)vinyl)-2-methoxy-phenol)] with improved stability and potent neuroprotective properties (Liu et al., 2008). Interestingly, CNB-001 corrected behavioral deficits in a rabbit ischemic stroke model (Lapchak et al., 2011). Furthermore, CeeTox analysis identified 183- to 643-fold in vitro efficacy/toxicity ratio, indicating broad therapeutic safety window (Lapchak and McKim, 2011). At the molecular level CNB-001 has been shown to positively affect protein kinase B (Akt) phosphorylation in HT-22 hippocampal neurons under ischemic conditions (Lapchak et al., 2011). Because Akt is a key regulator of insulin action and glucose uptake in mammals, this study was undertaken to determine the effects of the novel curcumin derivative CNB-001 on insulin signaling in both in vitro and in vivo models of insulin resistance.

Materials and Methods

CNB-001 was synthesized and characterized as previously described (Liu et al., 2008). 2-Deoxy-D-glucose-1-^{3}H, D-glucose, dimethylsulfoxide (DMSO), Oil Red O, propylene glycol, hematoxylin, and insulin were from Sigma-Aldrich (St. Louis, MO). Antibodies against glucose-regulated protein 78 (GRP78), GAPDH, phosphoreukaryotic initiation factor 2α (eIF2α), eIF2α, phospho-Akt, Akt, phosphoinsulin receptor (IR), IR, phosphor-IR substrate-1 [IRS-1 (Tyr^{1222})], IRS-1, and LumiGLO reagent were from Cell Signaling Technology (Boston, MA). Antibodies against protein-tyrosine phosphatase 1B (PTP1B) and anti-rabbit IgG were from Millipore (Billerica, MA). Dulbecco's modified Eagle's medium (DMEM), fetal bovine serum (FBS), horse serum, and MTT were from Invitrogen (Carlsbad, CA).

Cell Culture and Differentiation. A mouse muscle myoblasts cell line (C2C12) was obtained from American Type Culture Collection (Rockville, MD) and was cultured in DMEM supplemented with 10% fetal calf serum and 1% penicillin-streptomycin and incubated in an atmosphere of 95% O_2 and 5% CO_2 in air. After confluence, the culture medium was replaced with DMEM containing 2% horse serum to initiate myogenic differentiation (Nedachi and Kanzaki, 2006). After differentiation, myotubes were serum-free starved for 24 hours and then were subjected to various treatment described below.

Treatment of Cells. CNB-001 powder was dissolved in DMSO and added to the cultured cells, with a final solvent concentration in cell culture medium of 0.5%, which was used as a vehicle control in all the in vitro experiments. Insulin resistance was induced in C2C12 myotubes by treating them with palmitic acid (PA) (0.4 mM) for 12 hours. PA was prepared by conjugating it with bovine serum albumin as previously reported (Wang et al., 2006), and bovine serum albumin was included in the cell culture medium for every condition tested as a control. Cells were treated with 1 μM CNB-001 along with PA.

Cell Viability. MTT (1.2 mM) was added to C2C12 cells treated with different concentrations of CNB-001 and incubated for 4 hours. Medium was replaced with DMSO and incubated for 10 minutes. Absorbance was detected at 540 nm using SpectraMax 190 spectrophotometer (Molecular Devices, Sunnyvale, CA).

Western Blot Analysis. Cells were lysed in radioimmunoprecipitation assay lysis buffer followed by sonication and centrifugation at 14,000*g* for 15 minutes. Lysates (50 μg) in Laemmli sample buffer (Bio-Rad, Hercules, CA) were separated in 10% SDS-polyacrylamide gel electrophoresis. Subsequently, proteins were transferred to nitrocellulose membranes and incubated in the primary antibody against specific proteins. Following treatment with anti-rabbit or anti-mouse IgG horseradish peroxidase–linked antibody, immunoreactive bands were detected and quantified by enhanced chemiluminescence autoradiography by molecular imager Gel Doc XR+ System (Bio-Rad). All protein levels were normalized to GAPDH levels; phospho-eIF2α, -IR, -Akt, and -IRS-1 were normalized to corresponding total protein levels. Average values for control (untreated) group were used for normalization between different blots, when acquired ratios for controls were substantially different among the blots.

Glucose Uptake Assay. [^{3}H]-2-Deoxyglucose-uptake assay was performed as previously described (Kandadi et al., 2010). In brief, after serum starvation for 4 hours, C2C12 myotubes were washed with Krebs-Ringer phosphate HEPES buffer [KRPH buffer: 10 mM phosphate buffer (pH 7.4), 1 mM $MgSO_4$, 1 mM $CaCl_2$, 136 mM NaCl, 4.7 mM KCl, 10 mM HEPES (pH 7.6)] and then incubated without or with the test compound for 30 minutes at 37°C in the presence of 2-deoxy-[^{3}H]glucose (0.2 μCi). At the end of the incubation period, the cells were washed three times with ice-cold phosphate-buffered saline (PBS). The cells were then lysed in PBS containing 0.2 M NaOH, and glucose uptake was assessed by scintillation counting using Beckman LS5000TD liquid scintillation system (Beckman Coulter, Brea, CA). The counts were adjusted by the protein content or muscle weight.

Treatment of Animals. The experimental procedures described in this study were approved by the University of Wyoming Animal Use and Care Committee (Laramie, WY). C57BL6 mice were obtained from The Jackson Laboratory (Bar Harbor, ME). Seven-week-old adult males were randomly assigned to receive either low-fat diets (10 kcal% fat, 20 kcal% protein, 70 kcal% carbohydrate; Research Diets, New Brunswick, NJ) or high-fat diets (45 kcal% fat, 20 kcal% protein, 35 kcal% carbohydrate; Research Diets) for a period of 20 weeks. Each group was further assigned (n = 6) to receive either intraperitoneal injections of CNB-001 (40 mg/kg per day) or the vehicle (10% DMSO) every day for a period of 20 weeks, with the exception of weekends.

All mice were maintained with access to food and water ad libitum and were housed in the School of Pharmacy Animal Facility at the University of Wyoming at constant humidity and temperature with a light/dark cycle of 12 hours. Mice and food were weighed weekly every Friday, 24 hours after the last injection. Following metabolic and intraperitoneal insulin tolerance test (IPITT)/intraperitoneal glucose tolerance test (IPGTT) experiments, mice were allowed to recover on the same diet and injection regimen. On Tuesday, after 22 weeks of treatment and 24 hours after last injection, mice were fasted overnight and were injected intraperitoneally with insulin (0.75 IU/kg) and killed 30 minutes thereafter with ketamine/xylazine anesthesia (100:10 mg/kg), and internal organs, epididymal fat pads, and blood samples were collected. Tibia length was measured as a marker of body-size growth, because in extreme obesity conditions, body weight is not a reliable normalization factor due to excessive fat accumulation. Gastrocnemius muscle and liver tissues were homogenized in radioimmunoprecipitation assay lysis buffer (Upstate Biotechnology, Lake Placid, NY) using a PowerGen Homogenizer 125 (Thermo Fisher Scientific, Waltham, MA) and subsequently sonicated using Sonic Dismembrator 100 (Thermo Fisher Scientific). The homogenates were centrifuged at 14,000*g* for 15 minutes, and soluble fraction was used for protein expression analysis by Western blot as described above.

Metabolic Measurements. After 20 weeks of treatment, mice were housed individually in metabolic cages, acclimated for 24 hours to minimize the novelty effect, and then monitored for 24 hours in 12-hour light/dark cycle by indirect open-circuit calorimetry (Oxymax System; Columbus Instruments, Columbus, OH), as previously validated by different groups (Klaman et al., 2000; Escande et al.,

2010; Brown et al., 2012; Speakman, 2013). Studies were performed over the course of 5 days starting on Monday night. Mice were injected with the CNB-001 and vehicle, respectively, 12 hours before the beginning of the measurements and were not treated with the drug during 24 hours of monitoring. Diet feeding was maintained as described. Calibration of the calorimeter was performed at the beginning of each measurement day. Oxygen consumption and carbon dioxide production were measured by volume every 10 minutes. Respiratory exchange ratio (RER) was calculated as the ratio of V_{CO_2}/V_{O_2}. Energy expenditure was calculated as $(3.815 + 1.232 \times \text{RER}) \times V_{O_2}$ and normalized to body weight. Ambulatory movements were detected by infrared beams. Separate average values for light and dark phase of the day were calculated for each animal.

Intraperitoneal Glucose and Insulin Tolerance Tests. Mice were allowed to recover for 3 days after the last set of metabolic measurements. Diet feeding and injections were maintained as described before. After 21 weeks of drug treatment, IPGTT and IPITT were performed, respectively, in the morning, 24 hours after last CNB-001 injection. IPITT was performed on Tuesday morning after 21 weeks of treatment. Mice were allowed to recover for 2 days on the same diet and injection regimen. For IPGTT, mice were fasted overnight for 12 hours. Mice were weighed and then intraperitoneally injected with D-glucose (2 g/kg) for IPGTT or insulin (0.75 IU/kg) for IPITT. Glucose concentration in a drop of blood from cut tail vein was measured using Accu-Chek Advantage glucose meter (Roche, Manheim, Germany) at 0-, 30-, 60-, 90-, and 120-minute time points. Area under the curve (AUC) for each individual time curve was calculated using SigmaPlot statistical software (Jandel Scientific, San Rafael, CA).

Oil Red O Staining. Livers were frozen in Tissue-Tek O.C.T. Compound (Sakura Finetek, Torrance, CA). Fresh-frozen liver sections (8 μm) were fixed within ice-cold 10% formalin, washed with water, and placed in propylene glycol. Samples were stained in 0.5% Oil Red O solution in propylene glycol for 10 minutes at 60°C. After differentiating in 85% propylene glycol for 5 minutes, slides were rinsed in water and counterstained with hematoxylin. After mounting in VectMount AQ (Vector Laboratories, Burlingame, CA), liver samples were observed under the microscope.

Triglyceride, Interleukin-6, and Insulin Quantification. Liver and plasma triglycerides were determined by Triglyceride Assay Kit (BioVision, Milpitas, CA) following manufacturer protocol. Plasma interleukin (IL)-6 levels were measured using Mouse IL-6 ELISA Kit (Thermo Fisher Scientific) per manufacturer's protocol. Colorimetric assays were measured at 570 and 450 nm, respectively, on SpectraMax 190 spectrophotometer (Molecular Devices). Serum insulin content was investigated by using an ultrasensitive mouse insulin ELISA kit (Crystal Chem Inc., Downers Grove, IL) per manufacturer's instructions (Zong et al., 2011).

Ex Vivo Glucose-Uptake Assay. Gastrocnemius muscles were dissected out from mice, incubated for 30 minutes in Krebs-Henseleit buffer supplemented with 8 mM glucose and 0.1% bovine serum albumin in the presence or absence of CNB-001 in an atmosphere containing 95% O_2 and 5% CO_2. Glucose uptake was measured as described above, except that the muscle strips were freeze-dried, weighed, and treated with 1 N NaOH prior to determination of the radioactivity count.

Docking Simulation Study. All calculations were carried out with Discovery Studio 3.1 (Accelrys, San Diego, CA) on an Intel Xeon 5600 series. The crystal structure of PTP1B complexed to a reference ligand (Protein Data Bank code 3EB1) was used as a starting point. After removing the water and reference ligand, the protein was prepared with the standard protein-preparation protocol in Discovery Studio. The CNB-001 ligand was also built and prepared with Discovery Studio protocols. A cavity search was performed on the prepared protein to identify all possible sites in the protein structure that can accommodate a ligand. Seven possible cavities were determined by Discovery Studio. The prepared CNB-001 was docked in all cavities with CDOCKER. Only one out of the seven cavities identified could successfully accommodate the ligand. The conformation of docked ligand was minimized in situ with the In Situ Ligand Minimization protocol, and the ten lowest energy conformations were collected. The binding energies of the lowest energy conformations were calculated, and the conformation with the lowest binding energy was selected as the conformation most likely held by CNB-001 when complexed to PTP1B.

Statistical Analysis. Data are expressed as mean ± S.E.M. and statistically evaluated using one-way analysis of variance (ANOVA) followed by multiple comparisons test with Bonferroni correction using GraphPad Prism version 5.00 for Windows (GraphPad Software, Inc., San Diego, CA). For each individual IPGTT and IPITT curve, we used AUC measurement in GraphPad Prism based on trapezoid rule and reported total area under the curve for each treatment group as mean ± S.E.M.

Results

CNB-001 Rescues Cultured Myotubes From Palmitic Acid–Induced Insulin Resistance. The effect CNB-001 on insulin signaling was evaluated in C2C12 mouse skeletal muscle myotubes, as skeletal muscle is the predominant tissue that metabolizes glucose. Because CNB-001 has never been tested on C2C12 cells previously, we initially evaluated the potential cytotoxicity of the compound in cell culture medium to decide on a treatment concentration. By use of the MTT test to determine the effect of CNB-001 on cell viability, we identified the toxic concentration of CNB-001 that causes 50% cell death (TC_{50}) as 15.3 μM, whereas vehicle alone (0.5% DMSO) did not affect cell viability (Fig. 1A). In previous in vitro screening assays developed by CeeTox (Kalamazoo, MI), an effect of CNB-001 on rat hepatoma cell line (H4IIE) cell death was only observed with a much higher TC_{50} (193 μM), whereas the neuroprotection using HT22 cells was observed with an EC_{50} value in the range of 0.3–0.7 μM (Lapchak and McKim, 2011). The higher TC_{50} in our studies is attributable to the fact that we used quiescent cells that had been serum-starved for 24 hours, which may have already stressed the cells. The serum starving was essential for our studies as serum by itself has several growth factors that can affect insulin signaling. We used insulin-induced 2-deoxyglucose uptake as a measure of insulin sensitivity. Solvent alone did not have any effect on cellular glucose uptake in any of the tested conditions (Fig. 1B). As expected, insulin stimulation for 30 minutes resulted in more than a 2-fold increase of cellular glucose uptake compared with unstimulated cells; however, CNB-001 did not affect glucose uptake by myotubes even at the highest concentration (5 μM) tested in both unstimulated and insulin-stimulated cells (Fig. 1B). We next induced insulin resistance in the myotubes by treating them for 12 hours with palmitic acid (PA). As reported previously (Kandadi et al., 2011), PA treatment resulted in an attenuation of insulin-induced glucose uptake in cultured myotubes (Fig. 1B). Interestingly, CNB-001 supplementation under this insulin resistant condition restored glucose uptake (Fig. 1B). The reversal of PA-induced blunted glucose uptake by CNB-001 was concentration-dependent, and a near-complete recovery of glucose uptake was observed at 1 μM concentration of CNB-001. Because we did not find any significant difference in a glucose uptake between cells treated with either 1 or 5 μM CNB0001 (Fig. 1B), we used 1 μM for further experiments so as to avoid potential toxicity.

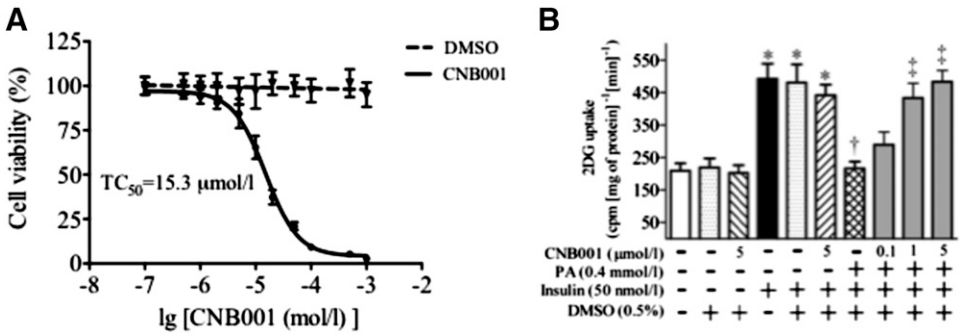

Fig. 1. CNB-001 reconciles palmitic acid-induced insulin resistance in cultured myotubes. (A) Cytotoxicity of CNB-001 was determined in quiescent C2C12 myotubes using MTT test ($n = 3$). Myotubes with 0.5% DMSO in cell culture media were used as a vehicle control. Data presented as a percentage of untreated control absorbance. TC_{50} of 15.3 μM was extrapolated from the graph (B) [^{3}H]2-Deoxyglucose-uptake assay ($n = 5$) in C2C12 myotubes, which were incubated with PA (0.4 mM) in the presence or absence of CNB-001 for 12 hours, and stimulated with insulin for 30 minutes (50 nM, 30 minutes). *$P < 0.05$ compared with corresponding no insulin conditions, †$P < 0.05$ compared with insulin stimulated cells, ‡$P < 0.05$ compared with PA + insulin treated cells.

CNB-001 Reconciles Blunted Insulin Signaling in Cultured Myotubes. Consistent with cellular glucose uptake data, we did not observe any effect of CNB-001 on insulin signaling under basal or insulin-stimulated conditions in C2C12 myotubes, as shown by Akt phosphorylation levels (Fig. 2, A and B). To understand the potential molecular mechanisms involved in the effects exhibited by CNB-001 on glucose uptake under insulin-resistant conditions, cultured C2C12 myotubes (following quiescence) were challenged with either PA or PA with CNB-001 for 12 hours, following which Western blot expression levels of IR, IRS-1, and Akt were evaluated. Western blot analysis revealed that under basal conditions neither PA nor CNB-001 altered the phosphorylation of IR, IRS-1, and Akt (Fig. 2, C–F). However, PA significantly attenuated insulin-stimulated phosphorylation of IR, IRS-1, and Akt, which was reversed by CNB-001.

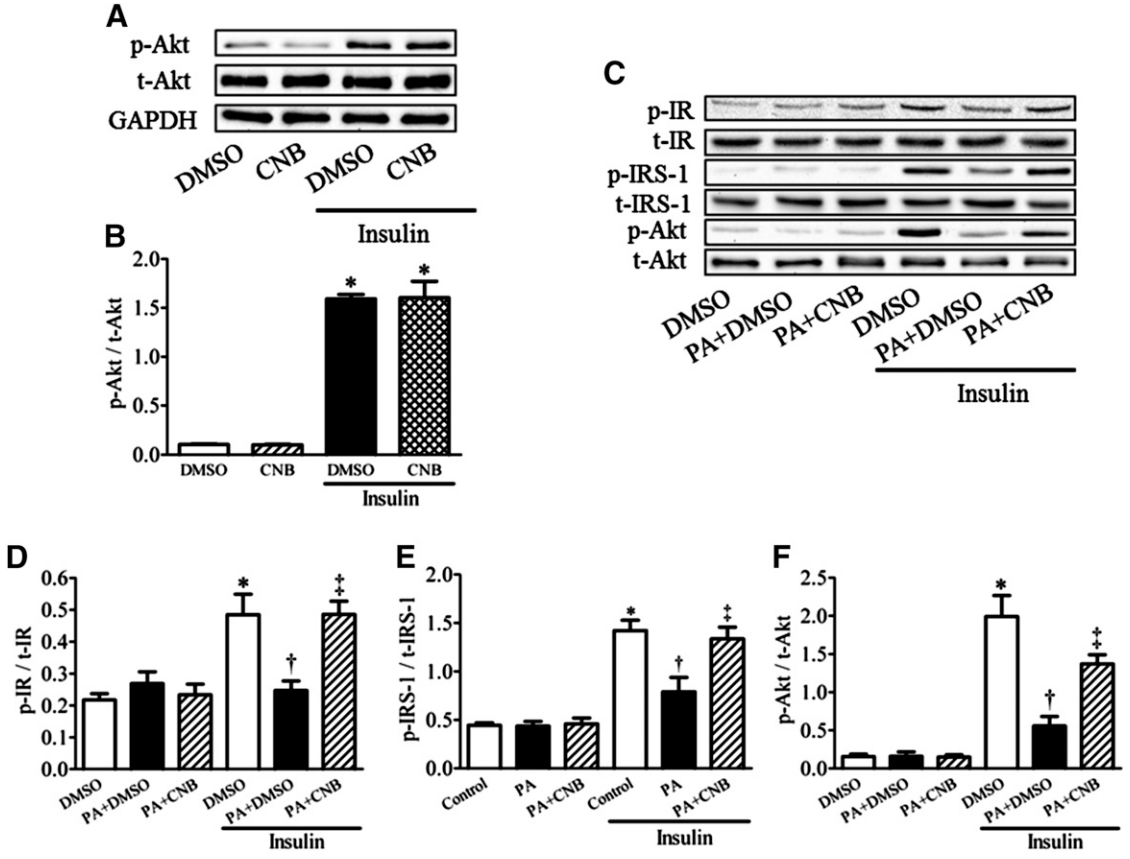

Fig. 2. Effect of CNB-001 on insulin-signaling pathway in palmitic acid–induced insulin resistance in cultured myotubes. Representative Western blots (A and C) and densitometric analysis ($n = 5$) of phospho-IR (D), phospho-IRS-1 (E), and phospho-Akt (B and F) protein levels in C2C12 myotubes under normal (A and B) or insulin resistant (C–F) conditions (0.4 mM PA) in a presence or absence of CNB-001 (1 μM) for 12 hours in basal and 30 minutes postinsulin (50 nM) treatment conditions.*$P < 0.05$ compared with corresponding no insulin conditions, †$P < 0.05$ compared with insulin stimulated cells, ‡$P < 0.05$ compared with PA + insulin treated cells.

Quantification of the blots indicates that CNB-001 causes a near complete reversal of IR and IRS-1 phosphorylation that was blunted by PA.

Effect of CNB-001 on Body Weight Gain and Adiposity in High-Fat Diet–Fed Mice. To investigate the possible effect of CNB-001 in vivo, we used the high-fat diet–induced obesity model in mice, a now standard model that many groups have successfully employed (Masuzaki et al., 2001; Sparks et al., 2005; Anderson et al., 2008; Kandadi et al., 2011; Hua et al., 2013; Xu et al., 2013). Mice subjected to a high-fat diet (HFD) gained significantly higher body weight in 20-weeks compared to mice on a normal diet (ND) (Fig. 3A; Table 1). In contrast, HFD-fed mice that received CNB-001 (40 mg/kg per day) for 20 weeks exhibited a significantly lower weight gain compared with those that received the vehicle. In mice that received the ND; however, CNB-001 did not affect body weight gain (Fig. 3A; Table 1). The analysis of average daily caloric intake for the 20-week period did not show a significant difference between treatment and groups (Fig. 3B), indicating that the weight loss induced by CNB-001 was not influenced by changes in food intake. Furthermore, CNB-001 injections in mice that received a normal diet failed to show any differences in the morphology of internal organs and organ weights, or in fasting glucose levels and plasma levels of triglycerides or inflammatory markers. In contrast, HFD-fed mice exhibited increased epididymal fat-pad mass, heart mass, heart-to-tibia-length ratio, liver mass, and liver-to-tibia-length ratio compared with those that received the normal diet (Table 1). CNB-001 supplementation for 20 weeks decreased overall adiposity, as well as heart and liver mass in HFD-fed mice (Table 1). Blood fasting glucose levels and serum triglycerides levels were increased in HFD group compared with ND group, which was attenuated by CNB-001 (Table 1). Elevated serum proinflammatory cytokine IL-6 in high-fat diet–fed mice was also attenuated by CNB-001 (Table 1).

Effect of CNB-001 and Energy Expenditure in Obese Mice. The decreased adiposity and resistance to diet-induced obesity in CNB-001-treated mice could result from decreased food consumption, fat malabsorption, or increased energy expenditure. Because CNB-001 attenuated body weight gain in high-fat diet–fed mice without altering food intake, we next investigated the impact of CNB-001 on energy metabolism in mice. The effect of CNB-001 on energy balance was assessed by monitoring the mice in open-circuit indirect calorimetry cages. Because mice are mostly active at night, data for rest (light phase) and active (dark phase) were separately calculated. Mice that received a high-fat diet showed decreased

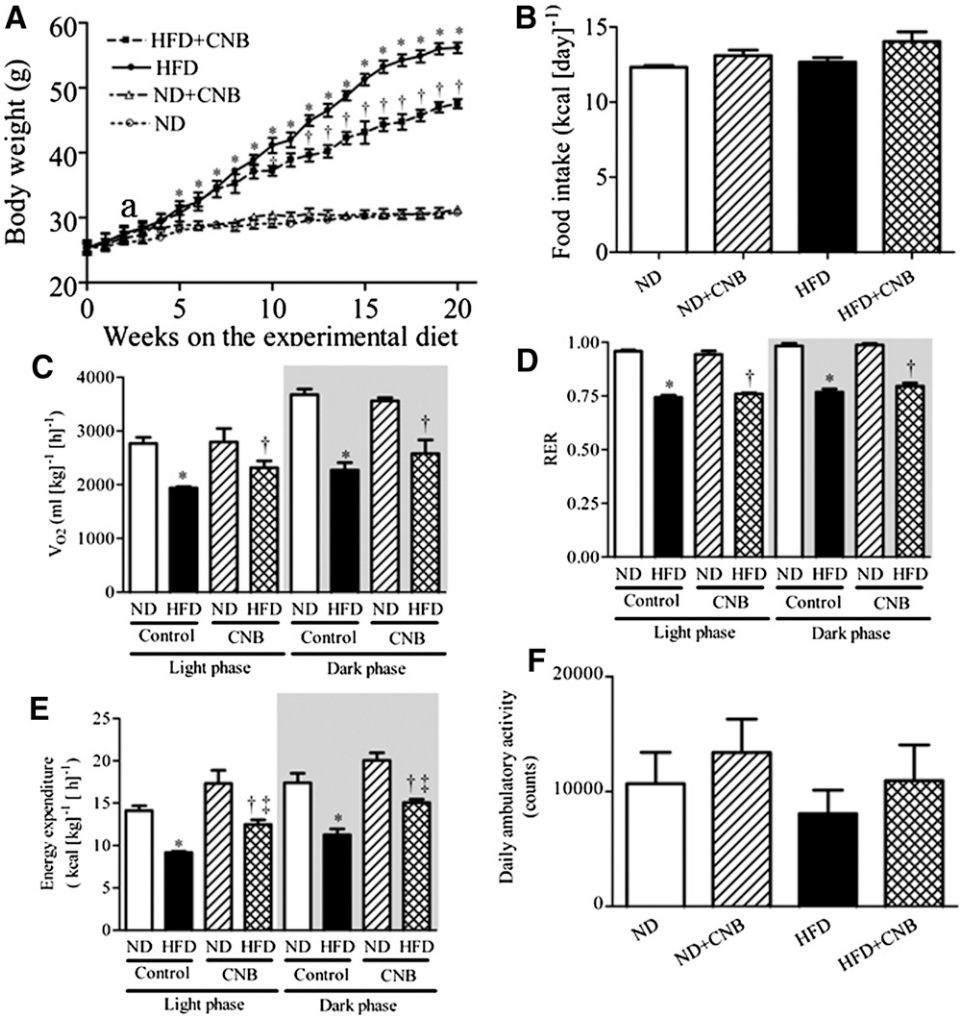

Fig. 3. CNB-001 protects against diet-induced obesity in mice. Change in body weight (A) and average daily caloric intake (B) for the 20-week period in C57BL/6J mice on ND or HFD received CNB-001 (ND+CNB and HFD+CNB) or vehicle injections for 20 weeks (n = 6 per group). *$P < 0.05$ compared with ND mice, †$P < 0.05$ compared with HFD mice. (C–F) Effect of long-term CNB-001 administration on oxygen consumption (C), RER (D), energy expenditure (E), and ambulatory physical activity (F) measured by open-circuit indirect calorimetry (n = 6). Activity data presented as total counts for 24 hours.*$P < 0.05$ compared with ND mice, †$P < 0.05$ compared with ND+CNB mice, ‡$P < 0.05$ compared with HFD mice.

TABLE 1
Morphometry and blood chemistry of fasted control and CNB-001-injected mice fed with a ND or a HFD for a 22-week period

Parameter	ND	ND+CNB	HFD	HFD+CNB
Body weight (g)	30.57 ± 0.53	31.47 ± 0.87	55.95 ± 1.41[a]	47.68 ± 0.77[b,c]
Tibia length (TL) (mm)	21.20 ± 0.27	20.55 ± 0.31	20.44 ± 0.31	20.46 ± 0.32
Epididymal fat pad (g)	0.48 ± 0.05	0.41 ± 0.07	2.36 ± 0.14[a]	1.92 ± 0.11[b,c]
Heart weight (HW) (mg)	163 ± 2	165 ± 10	220 ± 9[a]	193 ± 5[b,c]
HW/TL	7.73 ± 0.17	8.02 ± 0.42	10.76 ± 0.37[a]	9.55 ± 0.45[b,c]
Liver weight (LW) (g)	1.50 ± 0.12	1.55 ± 0.10	2.73 ± 0.22[a]	2.02 ± 0.06[b,c]
LW/TL	0.071 ± 0.006	0.075 ± 0.004	0.134 ± 0.006[a]	0.099 ± 0.004[b,c]
Kidney weight (KW) (g)	0.37 ± 0.02	0.37 ± 0.04	0.38 ± 0.01	0.40 ± 0.03
KW/TL	0.017 ± 0.001	0.018 ± 0.002	0.019 ± 0.001	0.019 ± 0.002
Fasting blood glucose (mg/dl)	74 ± 7	75 ± 5	194 ± 29[a]	107 ± 17[b,c]
Serum TG (mM)	0.93 ± 0.14	1.07 ± 0.04	1.77 ± 0.06[a]	1.29 ± 0.1[b,c]
Serum IL-6 (pg/ml)	201.1 ± 5.34	204.12 ± 13.6	561.2 ± 41.6[a]	319.3 ± 39.1[b,c]
Serum insulin (ng/ml)	0.55 ± 0.19	0.73 ± 0.19	13.29 ± 2.88[a]	8.58 ± 2.97[b]

[a] $P < 0.05$ compared with ND mice.
[b] $P < 0.05$ compared to ND+CNB mice.
[c] $P < 0.05$ compared to HFD mice.

O_2 consumption (VO_2) (Fig. 3C) as well as decreased respiratory exchange ratio (RER; Fig. 3D) at rest and active states, compared with those that received a normal diet, indicating fatty acid oxidation as a preferential energy source. CNB-001-treatment did not alter VO_2 and RER in either ND- and HFD-fed mice (Fig. 3, C and D). Energy expenditure tended to be higher in CNB-001-treated mice that were on a normal diet but did not reach statistical significance ($P > 0.05$). HFD-fed mice exhibited significantly lower energy expenditure compared with the normal diet–fed mice, which was partially reversed by CNB-001 (at both the rest and active states) (Fig. 3E). No effect of a diet or a genotype on physical activity was observed (Fig. 3F).

Effect of CNB-001 on High-Fat Diet–Induced Insulin Resistance and Glucose Intolerance. To study in vivo effects of CNB-001 administration, we performed IPGTT and IPITT to assess glucose tolerance and insulin sensitivity, respectively. As illustrated in Fig. 4, CNB-001 did not affect blood glucose levels in mice that received a normal diet in either the IPGTT (Fig. 4, A and B) or IPITT (Fig. 4, C and D). Additionally, basal serum insulin contents were not affected by CNB-001 as well (Table 1). High-fat feeding resulted in the development of severe glucose intolerance (Fig. 4A) and insulin resistance (Fig. 4C), characterized by increased area under the postchallenge blood glucose curves (Fig. 4, B and D), as well as a robust elevation in serum insulin levels (Table 1). Treatment with CNB-001 mitigated the effect of HFD feeding on blood-glucose disposal, as indicated by lower AUCs compared with that of the vehicle-treated group (Fig. 4, A–D). CNB-001 treatment also showed a trend toward lowering serum insulin levels (which were elevated in response to high-fat diet feeding), although this effect failed to reach statistical significance (Table 1). In addition to its effects on whole-body glucose disposal, we examined the effect of CNB-001 treatment on insulin-stimulated glucose uptake in skeletal muscle in normal and high-fat diet–fed mice (Fig. 4E). HFD-feeding resulted in significant muscle insulin resistance as evidenced by a significant attenuation (by ~5-fold) in insulin-stimulated glucose uptake in the gastrocnemius muscle. Treatment with CNB-001 restored insulin-stimulated glucose uptake in the skeletal muscle of HFD-fed mice (Fig. 4E), whereas it did not alter muscle glucose uptake in the mice that received normal diet.

CNB-001 Attenuates Hepatic Steatosis in Obese Mice. Because CNB-001 administration attenuated HFD-induced liver hypertrophy, we investigated the effect on CNB-001 on liver morphology. To this end, we used Oil Red O staining of the hepatic tissues to evaluate the extent of fat accumulation. As expected, HFD feeding for 20 weeks resulted in severe hepatic steatosis characterized by an increase in the number and size of fat droplets in the hepatocytes and lighter color of liver with visible white dots (Fig. 5A; Supplemental Fig. 1). Consistent with these observations, HFD-fed mice also exhibited elevated levels of hepatic triglycerides (Fig. 5B). The HFD diet–induced hepatic steatosis was mitigated by CNB-001 treatment, which restored color of liver back to normal red (Supplemental Fig. 1) and normalized fat droplet accumulation (Fig. 5A) and total triglycerides levels (Fig. 5B). As was the case with other parameters studies, CNB-001 had no effect on hepatic fat content in mice that received the normal diet.

Effect of CNB-001 on Insulin Signaling and Endoplasmic Reticulum Stress in Skeletal Muscle of Obese Mice. To explore the potential cellular mechanisms, we further investigated the insulin-signaling pathway in gastrocnemius muscle, a widely used skeletal muscle for obesity studies (Fig. 6, A–C). Insulin-stimulated phosphorylation levels of IR and Akt in skeletal muscles of mice subjected to high-fat feeding were significantly blunted compared with those that received a normal diet, indicating overt insulin resistance (Fig. 6, A–C). Administration of CNB-001 partially restored insulin-induced phosphorylation of both IR (Fig. 6B) and Akt (Fig. 6C) in the high-fat diet–fed mice. We also evaluated the expression levels of the negative regulator of insulin-signaling protein tyrosine phosphatase 1B (PTP1B). Skeletal muscle of HFD-fed mice had higher levels of PTP1B expression (Fig. 6, A and D). Interestingly, CNB00 treatment normalized PTP1B expression in HFD-fed mice (Fig. 6, A and D), which may have contributed to the beneficial effects of CNB-001. CNB-001 did not alter PTP1B expression levels in mice that received a normal diet. Because endoplasmic reticulum stress has been implicated as a common pathway involved in high-fat diet–induced insulin resistance, we next evaluated the effect of CNB-001 treatment on the extent of ER stress in the gastrocnemius muscle (Fig. 6, A, E,and F). Similar results in terms of effect of CNB-001 on insulin signaling and PTP1B expression were obtained in liver

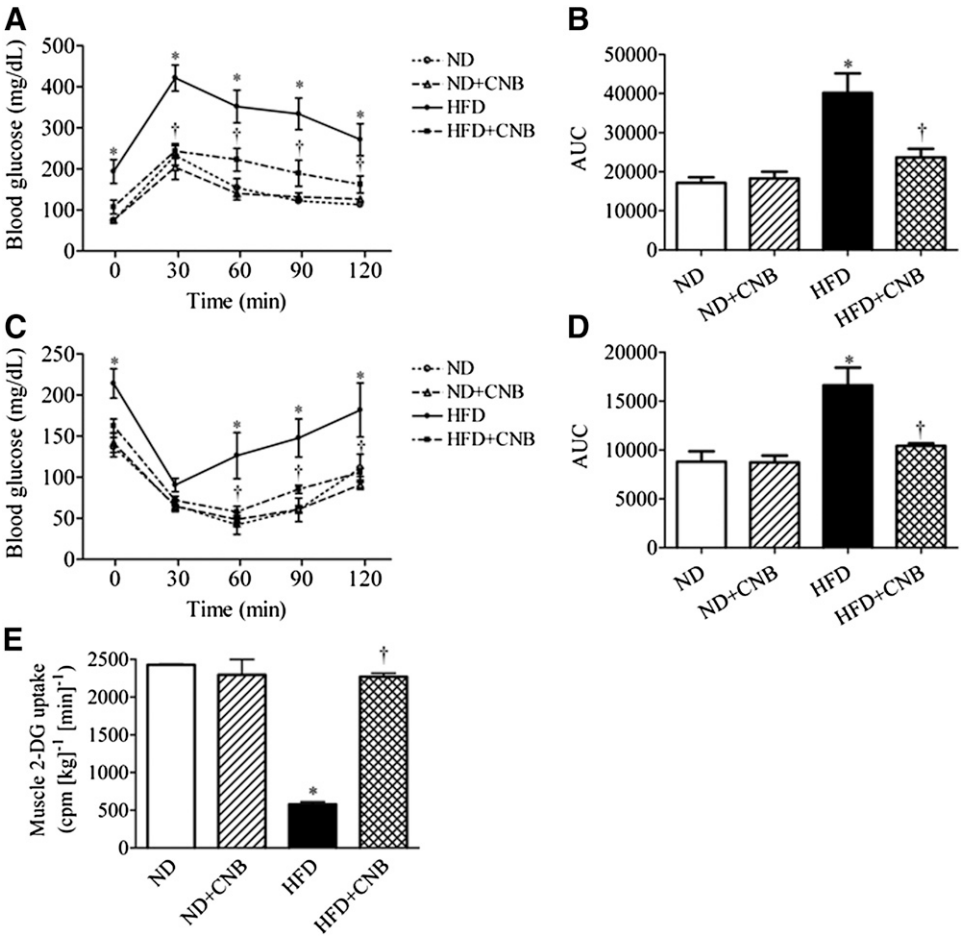

Fig. 4. CNB-001 administration improves diet-induced insulin resistance and skeletal muscle glucose uptake in mice. IPGTT (A) and IPITT (C) for C57BL/6J mice on a normal or high-fat content diet that received CNB-001 (ND+CNB and HFD +CNB) or vehicle injections for 21 weeks (n = 6). AUC for each individual curve of IPGTT (B) and IPITT (D) was calculated. (E) [^{3}H]2-Deoxyglucose-uptake assay (n = 6) in gastrocnemius muscles of mice challenged with insulin for 30 minutes after 22 weeks of the experiment. *$P < 0.05$ compared with ND mice, †$P < 0.05$ compared with HFD mice.

samples (data not shown). As expected, HFD-fed mice had elevated levels of ER-stress markers GRP78 and phospho-eIF2α (Fig. 6, E and F, respectively). Whereas CNB-001 administration decreased phosphorylation levels of eIF2α in high-fat diet–fed mice (Fig. 6F), expression levels of GRP78 remained unchanged (Fig. 6E). Extent of ER stress in gastrocnemius muscle of mice that received a normal diet remained unchanged with CNB-001 treatment.

Binding of CNB-001 in the Active Site of PTP1B. To further evaluate the effect of CNB-001 on PTP1B, an in silico molecular-docking study was performed (Fig. 7). The modeling suggests that CNB-001 can be accommodated into the active site cleft of PTP1B crystal structure (Fig. 7A), and the hydrogen bond can be formed between the phenolic oxygen of the CNB-001 and the thiol group of catalytic Cys215 residue at a distance of 2.98 Å (Fig. 7B). In addition, two hydrogen bonds may be formed between the phenolic oxygen of the CNB-001 and Ala217 (at 3.07 Å), as well as between hydrogen of 1*H*-pyrazoyl moiety and Asp48 (at 2.09 Å). Additionally, the phenyl ring in the 1-phenyl-1*H*-pyrazoyl moiety of CNB-001 allows for an orientation toward Arg24, enabling a π-interaction (Fig. 7B).

Discussion

The major findings from our study are: 1) The novel neuroprotective and neurotrophic agent CNB-001 protects against high-fat diet–induced weight gain and fat accumulation, 2) CNB-001 treatment increases energy expenditure and alleviates high-fat diet–induced insulin resistance and glucose intolerance, 3) CNB-001 administration augments phosphorylation of IR and Akt under insulin resistance conditions both in vitro and in vivo, and 4) CNB-001 attenuates high-fat diet–induced expression of PTP1B and phospho-eIF2α in vivo.

In these studies, we focused on a novel neurotrophic curcumin derivative, CNB-001, as a candidate molecule to improve glucose homeostasis and insulin sensitivity in a mouse model of obesity. Our data demonstrate that CNB-001 administration prevents body weight gain associated with HFD feeding. High-fat diet–fed mice that received CNB-001 also had smaller deposition of adipose tissue and lower levels of serum triglycerides. Increase in energy expenditure in response to CNB-001 treatment in high-fat diet–fed mice may be a plausible explanation for the reduced weight gain in these animals. In normal diet–fed mice CNB-001 treatment also seemed to increase energy expenditure, but the difference did not reach statistical significance and was not accompanied by a change in body weight. There could be several explanations for this effect. First, our energy expenditure data has certain limitations. Energy expenditure was normalized to body weight, which is a widely used method to account for difference in animal size (Tschop et al., 2012). However, this method often creates spurious results, because it does not account for difference in metabolic rates for various tissues and overcompensates for the mass effect (Speakman, 2013). Division by fat-free mass seems to be a better approach, but

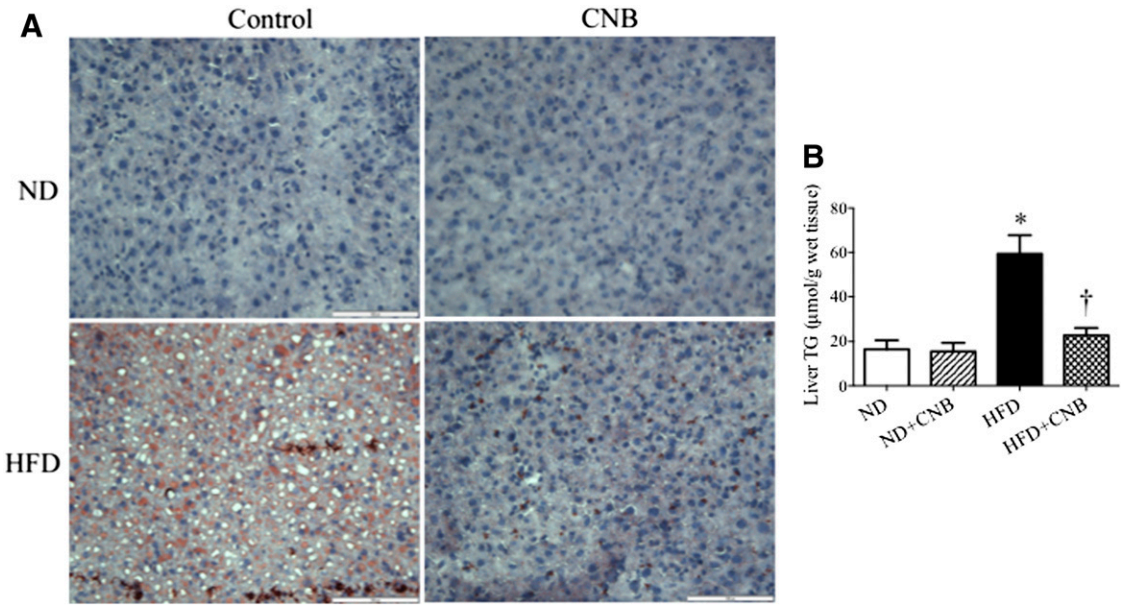

Fig. 5. CNB-001 administration protects against diet-induced hepatic steatosis in mice. Analysis of liver fat content ($n = 6$) with Oil Red O staining (A) and total triglyceride ELISA kit (B) in C57BL/6J mice on normal or high-fat content diets that received CNB-001 (ND+CNB and HFD+CNB) or vehicle injections for 22 weeks. Red staining, fat droplets; blue, nuclei. Scale bar, 100 μm. *$P < 0.05$ compared with ND mice, †$P < 0.05$ compared with HFD mice.

lean mass analysis technique was not available at the time of the experiments were performed. In addition, the difference in metabolic rates could be completely accounted for by the difference in liver size (Selman et al., 2001). Thus, the effect of CNB-001 on liver size in high-fat diet–fed mice but not in normal diet–fed mice might explain the significant difference in energy expenditure observed in the obese but not in the control group. The decreased body weights of obese mice that received CNB-001 could also be explained possibly by changes in adipogenesis and/or lipogenesis, rather than energy expenditure, and requires further investigations. We also could not rule out malabsorption of excessive dietary fat by high-fat diet–fed mice upon CNB-001 administration.

Furthermore, CNB-001 administration improved whole-body glucose disposal rate in both IPGTT and IPITT. These effects may be attributed to the ability of CNB-001 to augment insulin signaling both in vivo and in vitro, which was evidenced by its ability to improve the phosphorylation of IR and

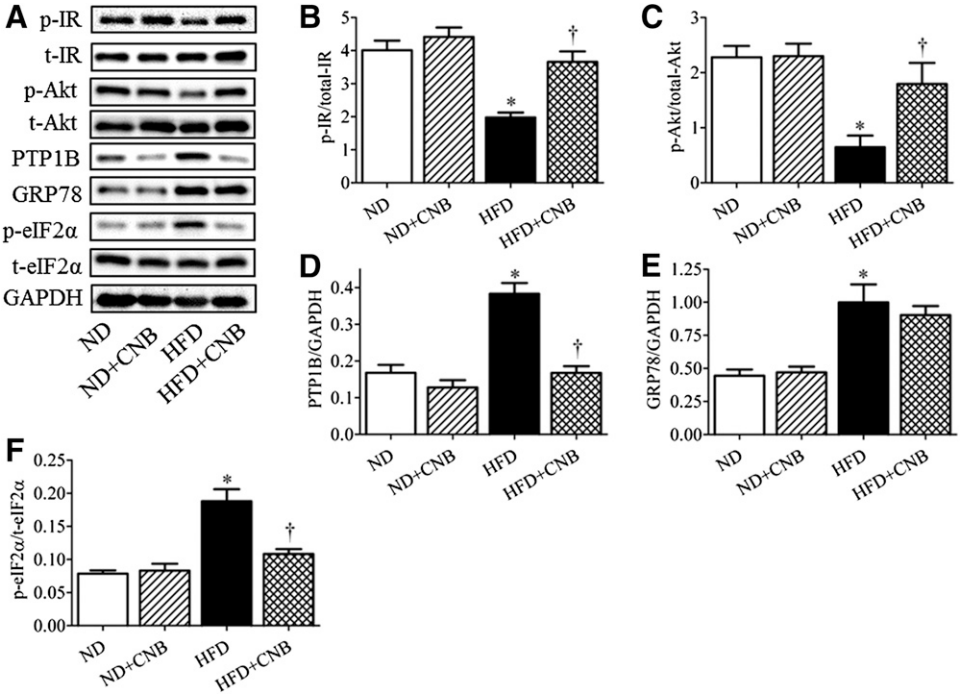

Fig. 6. The effect of CNB-001 on insulin-signaling pathway and endoplasmic reticulum stress in diet-induced model of obesity in mice. C57BL/6J mice on a normal or high-fat content diet, received CNB-001 (ND+CNB and HFD+CNB) or vehicle injections for 22 weeks, were challenged with insulin for 30 minutes, and sacrificed and gastrocnemius muscles were collected. Representative Western blots (A) and densitometric analysis ($n = 6$) of phospho-IR (B), phospho-Akt (C), PTP1B (D), GRP78 (E), and phospho-eIF2α (F) protein expression are shown. *$P < 0.05$ compared with ND mice, †$P < 0.05$ compared with HFD mice.

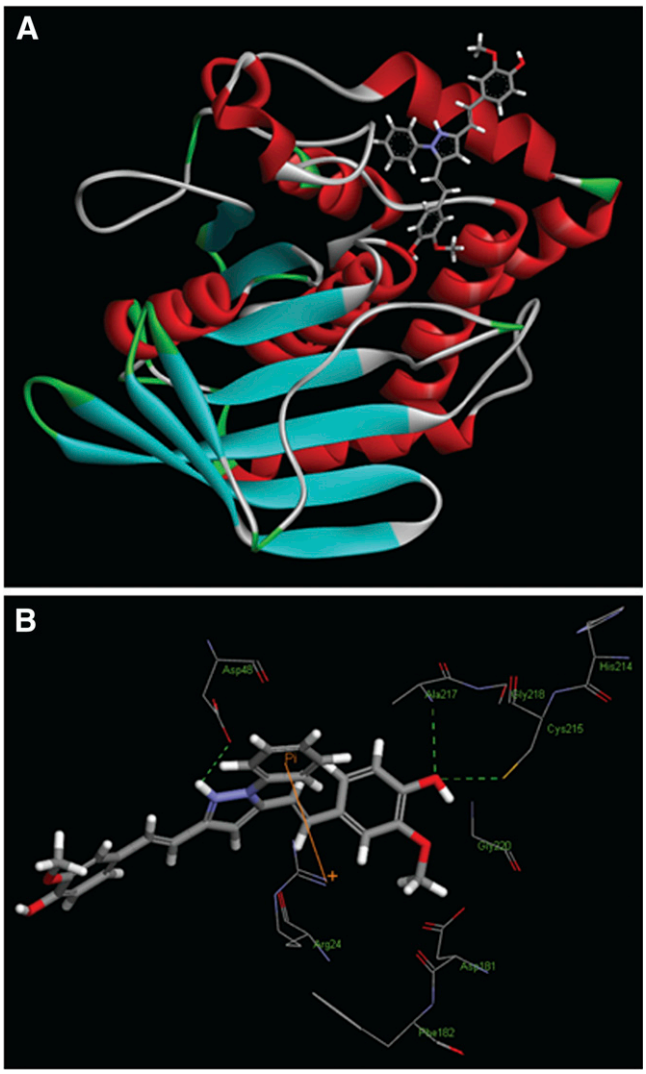

Fig. 7. CNB-001 docked into an active site of PTP1B. (A) Binding model of CNB-001 shown in ball and stick in the active site of PTP1B (red, α-helix; blue, β-strand; green, β-turns; gray, disordered regions). (B) Expanded view showing the interactions between CNB-001 and the amino acids residues of PTP1B.

Akt phosphorylation under insulin-resistant conditions. This augmentation of insulin signaling was associated with an increase in glucose uptake both in cultured myotubes and in skeletal muscle of the high-fat diet–fed mice. A large body of evidence supports a complex interplay between type 2 diabetes and the pathophysiology of nonalcoholic fatty liver disease (Williams et al., 2013). We found excessive lipid accumulation in the liver of mice that received a high-fat diet and elevated levels of hepatic triglycerides, which was negated by CNB-001.

Binding of insulin to the transmembrane insulin receptors results in the phosphorylation of the β subunit of the insulin receptor, which functions as a kinase leading to the phosphorylation of IRS-1, which leads to the recruitment and activation of signaling pathways, including the Ras/mitogen-activated protein kinase and phosphatidylinositol 3-kinase/Akt pathways that mediate the metabolic, transcriptional, and mitogenic actions of insulin. By virtue of these signaling actions insulin regulates glucose homeostasis in the liver, muscle, and adipose tissues by promoting glucose uptake and glycogen synthesis and inhibiting glycogenolysis and gluconeogenesis (Litherland et al., 2001). Several previous studies have suggested that PTP1B is a phosphatase that targets the tyrosine-phosphorylated insulin receptor β and IRS-1 and thereby functions as a negative regulator of insulin signaling (Kenner et al., 1996; Asante-Appiah and Kennedy, 2003). Deletion of PTP1B results in improved insulin sensitivity and glucose tolerance, suggesting that PTP1B is a potential target for therapeutic intervention in insulin resistant conditions (Elchebly et al., 1999). Therefore, we evaluated the effects of CNB-001 on PTP1B expression, the well-known negative regulator of insulin signaling and possible link between obesity and development of insulin resistance. Consistent with previous observations in our laboratory and by others (Zabolotny et al., 2008; Panzhinskiy et al., 2013) PTP1B expression was elevated in the skeletal muscle of high-fat diet–fed mice. Whereas CNB-001 treatment upregulated the kinases in the insulin-signaling pathway, it induced a reciprocal downregulation of PTP1B expression, which helps further substantiate the claim that CNB-001 may be mediating its effects by augmenting the insulin-signaling pathway. These results are consistent with findings of Li and colleagues (2010), who recently showed that curcumin was able to inhibit hepatic PTP1B. Furthermore, CNB-001 inhibition of PTP1B may also explain its ability to increase energy expenditure, as PTP1B knockout mice have been shown to have increased metabolic rate (Klaman et al., 2000; Narumoto et al., 2012). Interestingly, data from Elchebly et al. (1999) and our laboratory (Panzhinskiy et al., 2013) showed that PTP1B knockout reduced body weight in mice receiving high-fat content diet, but not control chow, which is consistent with the effect of CNB-001 treatment on body weight only in high-fat diet–fed mice. Our docking simulation studies confirmed that CNB-001 can bind and potentially inhibit PTP1B, and thus the effects of CNB-001 administration on insulin resistance, adiposity, weight gain, and glucose metabolism in obese mice can be attributed to PTP1B inhibition, as seen in the case of other reported inhibitors of PTP1B (Lantz et al., 2010; Ma et al., 2011). For example, a recent study showed that novel proteoglycan PTP1B inhibitor FYGL decreased the plasma glucose level by the mechanism of inhibiting PTP1B expression and activity, consequently regulating the tyrosine phosphorylation level of the IR-β subunit and the level of hepatic glycogen, thus resulting in improved of insulin sensitivity in *db/db* mice (Wang et al., 2012). However, we cannot exclude the possibility that CNB-001 may target proteins or pathways that regulate the expression of PTP1B and/or a variety of other pathways that mediate insulin resistance, such as those involved in the metabolism of fatty acid.

Accumulating evidence has demonstrated that activation of multiple branches of ER stress response represents a common pathway in pathogenesis of obesity, insulin resistance, and type 2 diabetes (Ozcan et al., 2004). In our study, we found increased expression of ER stress markers GRP78 and phospho-eIF2α in skeletal muscle following high-fat diet feeding. Administration of CNB-001 normalized the phosphorylation of eIF2α without affecting GRP78 expression. This differential regulation of ER stress may be explained by changes in PTP1B levels, as we have seen (in our previous studies) that absence of PTP1B in vitro and in vivo results in impaired phosphorylation of eIF2α but not GRP78 activation during ER stress response (Panzhinskiy et al., 2013).

Collectively, our data demonstrate that CNB-001 alleviates insulin resistance and prevents body weight gain associated with high-fat diet. In addition, hepatic steatosis associated with obesity was attenuated by CNB-001. Additionally, phospho-eIF2α and PTP1B, which are elevated in obesity, are down-regulated by CNB-001. Nonetheless, given the low TC_{50} value of the CNB-001, the likelihood that the observed beneficial effects may represent a toxic manifestation cannot be completely ruled out. Taken together, CNB-001 may represent a promising drug candidate for future development as a treatment of obesity-induced insulin resistance and associated complications.

Authorship Contributions

Participated in research design: Panzhinskiy, Lehmann, Ren, Nair.
Conducted experiments: Panzhinskiy, Hua, Topchiy.
Performed data analysis: Panzhinskiy.
Wrote or contributed to the writing of the manuscript: Panzhinskiy.

References

Aggarwal BB, Sundaram C, Malani N, and Ichikawa H (2007) Curcumin: the Indian soil gold. *Adv Exp Med Biol* **595**:1–75.

Alappat L and Awad AB (2010) Curcumin and obesity: evidence and mechanisms. *Nutr Rev* **68**:729–738.

Anand P, Kunnumakkara AB, Newman RA, and Aggarwal BB (2007) Bioavailability of curcumin: problems and promises. *Mol Pharm* **4**:807–818.

Anderson SR, Gilge DA, Steiber AL, and Previs SF (2008) Diet-induced obesity alters protein synthesis: tissue-specific effects in fasted versus fed mice. *Metabolism* **57**: 347–354.

Asante-Appiah E and Kennedy BP (2003) Protein tyrosine phosphatases: the quest for negative regulators of insulin action. *Am J Physiol Endocrinol Metab* **284**: E663–E670.

Bahrami H, Bluemke DA, Kronmal R, Bertoni AG, Lloyd-Jones DM, Shahar E, Szklo M, and Lima JA (2008) Novel metabolic risk factors for incident heart failure and their relationship with obesity: the MESA (Multi-Ethnic Study of Atherosclerosis) study. *J Am Coll Cardiol* **51**:1775–1783.

Balasubramanyam K, Varier RA, Altaf M, Swaminathan V, Siddappa NB, Ranga U, and Kundu TK (2004) Curcumin, a novel p300/CREB-binding protein-specific inhibitor of acetyltransferase, represses the acetylation of histone/nonhistone proteins and histone acetyltransferase-dependent chromatin transcription. *J Biol Chem* **279**:51163–51171.

Brown JD, Naples SP, and Booth FW (2012) Effects of voluntary running on oxygen consumption, RQ, and energy expenditure during primary prevention of diet-induced obesity in C57BL/6N mice. *J Appl Physiol (1985)* **113**:473–478.

Elchebly M, Payette P, Michaliszyn E, Cromlish W, Collins S, Loy AL, Normandin D, Cheng A, Himms-Hagen J, and Chan CC, et al. (1999) Increased insulin sensitivity and obesity resistance in mice lacking the protein tyrosine phosphatase-1B gene. *Science* **283**:1544–1548.

Escande C, Chini CCS, Nin V, Dykhouse KM, Novak CM, Levine J, van Deursen J, Gores GJ, Chen J, and Lou Z, et al. (2010) Deleted in breast cancer-1 regulates SIRT1 activity and contributes to high-fat diet-induced liver steatosis in mice. *J Clin Invest* **120**:545–558.

Hua Y, Zhang Y, Dolence J, Shi G-P, Ren J, and Nair S (2013) Cathepsin K knockout mitigates high-fat diet-induced cardiac hypertrophy and contractile dysfunction. *Diabetes* **62**:498–509.

Kahn BB and Flier JS (2000) Obesity and insulin resistance. *J Clin Invest* **106**: 473–481.

Kandadi MR, Rajanna PK, Unnikrishnan MK, Boddu SP, Hua Y, Li J, Du M, Ren J, and Sreejayan N (2010) 2-(3,4-Dihydro-2H-pyrrolium-1-yl)-3oxoindan-1-olate (DHPO), a novel, synthetic small molecule that alleviates insulin resistance and lipid abnormalities. *Biochem Pharmacol* **79**:623–631.

Kandadi MR, Unnikrishnan MK, Warrier AK, Du M, Ren J, and Sreejayan N (2011) Chromium (D-phenylalanine)3 alleviates high fat-induced insulin resistance and lipid abnormalities. *J Inorg Biochem* **105**:58–62.

Kenner KA, Anyanwu E, Olefsky JM, and Kusari J (1996) Protein-tyrosine phosphatase 1B is a negative regulator of insulin- and insulin-like growth factor-I-stimulated signaling. *J Biol Chem* **271**:19810–19816.

Klaman LD, Boss O, Peroni OD, Kim JK, Martino JL, Zabolotny JM, Moghal N, Lubkin M, Kim YB, and Sharpe AH, et al. (2000) Increased energy expenditure, decreased adiposity, and tissue-specific insulin sensitivity in protein-tyrosine phosphatase 1B-deficient mice. *Mol Cell Biol* **20**:5479–5489.

Lantz KA, Hart SGE, Planey SL, Roitman MF, Ruiz-White IA, Wolfe HR, and McLane MP (2010) Inhibition of PTP1B by trodusquemine (MSI-1436) causes fat-specific weight loss in diet-induced obese mice. *Obesity (Silver Spring)* **18**: 1516–1523.

Lapchak PA and McKim JM, Jr (2011) CeeTox^{TM} analysis of CNB-001 a novel curcumin-based neurotrophic/neuroprotective lead compound to treat stroke: comparison with NXY-059 and radicut. *Transl Stroke Res* **2**:51–59.

Lapchak PA, Schubert DR, and Maher PA (2011) Delayed treatment with a novel neurotrophic compound reduces behavioral deficits in rabbit ischemic stroke. *J Neurochem* **116**:122–131.

Li J-M, Li Y-C, Kong L-D, and Hu Q-H (2010) Curcumin inhibits hepatic protein-tyrosine phosphatase 1B and prevents hypertriglyceridemia and hepatic steatosis in fructose-fed rats. *Hepatology* **51**:1555–1566.

Litherland GJ, Hajduch E, and Hundal HS (2001) Intracellular signalling mechanisms regulating glucose transport in insulin-sensitive tissues (review). review *Mol Membr Biol* **18**:195–204.

Liu Y, Dargusch R, Maher P, and Schubert D (2008) A broadly neuroprotective derivative of curcumin. *J Neurochem* **105**:1336–1345.

Ma YM, Tao RY, Liu Q, Li J, Tian JY, Zhang XL, Xiao ZY, and Ye F (2011) PTP1B inhibitor improves both insulin resistance and lipid abnormalities *in vivo* and *in vitro*. *Mol Cell Biochem* **357**:65–72.

Masuzaki H, Paterson J, Shinyama H, Morton NM, Mullins JJ, Seckl JR, and Flier JS (2001) A transgenic model of visceral obesity and the metabolic syndrome. *Science* **294**:2166–2170.

Narumoto O, Matsuo Y, Sakaguchi M, Shoji S, Yamashita N, Schubert D, Abe K, Horiguchi K, Nagase T, and Yamashita N (2012) Suppressive effects of a pyrazole derivative of curcumin on airway inflammation and remodeling. *Exp Mol Pathol* **93**:18–25.

Nedachi T and Kanzaki M (2006) Regulation of glucose transporters by insulin and extracellular glucose in C2C12 myotubes. *Am J Physiol Endocrinol Metab* **291**: E817–E828.

Ogden CL, Yanovski SZ, Carroll MD, and Flegal KM (2007) The epidemiology of obesity. *Gastroenterology* **132**:2087–2102.

Ozcan U, Cao Q, Yilmaz E, Lee AH, Iwakoshi NN, Ozdelen E, Tuncman G, Görgün C, Glimcher LH, and Hotamisligil GS (2004) Endoplasmic reticulum stress links obesity, insulin action, and type 2 diabetes. *Science* **306**:457–461.

Panzhinskiy E, Hua Y, Culver B, Ren J, and Nair S (2013) Endoplasmic reticulum stress upregulates protein tyrosine phosphatase 1B and impairs glucose uptake in cultured myotubes. *Diabetologia* **56**:598–607.

Selman C, Lumsden S, Bünger L, Hill WG, and Speakman JR (2001) Resting metabolic rate and morphology in mice (Mus musculus) selected for high and low food intake. *J Exp Biol* **204**:777–784.

Seo K-I, Choi M-S, Jung UJ, Kim H-J, Yeo J, Jeon S-M, and Lee M-K (2008) Effect of curcumin supplementation on blood glucose, plasma insulin, and glucose homeostasis related enzyme activities in diabetic *db/db* mice. *Mol Nutr Food Res* **52**: 995–1004.

Shao W, Yu Z, Chiang Y, Yang Y, Chai T, Foltz W, Lu H, Fantus IG, and Jin T (2012) Curcumin prevents high fat diet induced insulin resistance and obesity via attenuating lipogenesis in liver and inflammatory pathway in adipocytes. *PLoS ONE* **7**:e28784.

Sparks LM, Xie H, Koza RA, Mynatt R, Hulver MW, Bray GA, and Smith SR (2005) A high-fat diet coordinately downregulates genes required for mitochondrial oxidative phosphorylation in skeletal muscle. *Diabetes* **54**:1926–1933.

Speakman JR (2013) Measuring energy metabolism in the mouse – theoretical, practical and analytical considerations. *Frontiers in Physiology* **4**.

Tschöp MH, Speakman JR, Arch JR, Auwerx J, Brüning JC, Chan L, Eckel RH, Farese RV, Jr, Galgani JE, and Hambly C, et al. (2012) A guide to analysis of mouse energy metabolism. *Nat Methods* **9**:57–63.

Wang C-D, Teng B-S, He Y-M, Wu J-S, Pan D, Pan L-F, Zhang D, Fan Z-H, Yang H-J, and Zhou P (2012) Effect of a novel proteoglycan PTP1B inhibitor from *Ganoderma lucidum* on the amelioration of hyperglycaemia and dyslipidaemia in *db/db* mice. *Br J Nutr* **108**:2014–2025.

Wang XL, Zhang L, Youker K, Zhang MX, Wang J, LeMaire SA, Coselli JS, and Shen YH (2006) Free fatty acids inhibit insulin signaling-stimulated endothelial nitric oxide synthase activation through upregulating PTEN or inhibiting Akt kinase. *Diabetes* **55**:2301–2310.

Williams KH, Shackel NA, Gorrell MD, McLennan SV, and Twigg SM (2013) Diabetes and nonalcoholic fatty liver disease: a pathogenic duo. *Endocr Rev* **34**: 84–12.

Xu X, Hua Y, Nair S, Zhang Y, and Ren J (2013) Akt2 knockout preserves cardiac function in high-fat diet-induced obesity by rescuing cardiac autophagosome maturation. *J Mol Cell Biol* **5**:61–63.

Zabolotny JM, Kim YB, Welsh LA, Kershaw EE, Neel BG, and Kahn BB (2008) Protein-tyrosine phosphatase 1B expression is induced by inflammation in vivo. *J Biol Chem* **283**:14230–14241.

Zong H, Wang CC, Vaitheesvaran B, Kurland IJ, Hong W, and Pessin JE (2011) Enhanced energy expenditure, glucose utilization, and insulin sensitivity in VAMP8 null mice. *Diabetes* **60**:30–38.

Address correspondence to: Dr. Sreejayan Nair, University of Wyoming, School of Pharmacy and the Center for Cardiovascular Research and Alternative Medicine, 1000 E. University Avenue, Department 3375, Laramie, WY 82071. E-mail address: sreejay@uwyo.edu